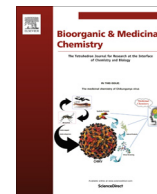




Contents lists available at ScienceDirect

Bioorganic & Medicinal Chemistry

journal homepage: www.elsevier.com/locate/bmc

Synthesis and diabetic neuropathic pain-alleviating effects of 2*N*-(pyrazol-3-yl)methylbenzo[*d*]isothiazole-1,1-dioxide derivatives

Jin Ri Hong^{b,c}, Young Jin Choi^{b,c}, Gyochang Keum^{a,b}, Ghilsoo Nam^{a,b,*}

^a Center for Neuro-Medicine, Brain Science Institute, Korea Institutes of Science and Technology (KIST), Seoul 02792, Republic of Korea

^b Division of Bio-Medical Sciences & Technology, KIST School, Korea University of Science and Technology (UST), Gajungro 217, Yuseong-gu, Daejeon 305-350, Republic of Korea

ARTICLE INFO

Article history:

Received 11 May 2017

Revised 4 July 2017

Accepted 6 July 2017

Available online xxxxx

Keywords:

T-type calcium channel inhibition

Fused-benzosulfonamides

Neuropathic pain

Allodynia

ABSTRACT

A novel series of fused-benzosulfonamide 2-*N*-(pyrazol-3-yl)methylbenzo[*d*]isothiazole-1,1-dioxide derivatives was designed and synthesized as metabolically stable T-type calcium channel inhibitors. Several compounds, **9**, **10**, and **17**, displayed potent T-type channel inhibitory activity. Among them, compounds **10** and **17** showed good metabolic stability in human liver microsomes, and low hERG channel and CYP450 inhibition. Compound **10** exhibited diabetic neuropathic pain-alleviating effects in a streptozotocin-induced peripheral diabetic neuropathy (PDN) model. The maximum efficacy of compound **10**, which was 3-fold more potent than gabapentin, was observed at 1 h after administration, and co-administration of compound **10** with gabapentin showed a considerable synergic effect.

© 2017 Published by Elsevier Ltd.

1. Introduction

Peripheral neuropathy is one of the most common complications of early onset type 1 diabetes mellitus. Over 60% of diabetes patients suffering from peripheral diabetic neuropathy (PDN) also experience neuropathic pain.¹ Current therapies for treating painful PDN are limited and associated with serious side effects and addiction. Treatment of PDN is still based on pathogenic mechanisms and symptomatic pain management, as well as clinically recommended therapeutic agents such as antidepressants, γ -aminobutyric acid analogues, opioids, and topical agents. There are currently only three Food and Drug Administration (FDA)-approved PDN drugs: duloxetine (approved in 2004), pregabalin (approved in 2004), and tapentadol (approved in 2012) (Fig. 1).²

Although the precise cellular mechanism of painful PDN is not clearly understood, several recent studies have reported that the α_{1H} subtype of the T-type calcium channel plays an important role in the hyper-excitability of small- and medium-sized dorsal root ganglion (DRG) cells, resulting in painful PDN symptoms.³ The selective T-type calcium channel blocker, (3 β ,5 α ,17 β)-17-hydroxyestrane-3-carbonitrile (ECN), alleviates hyperalgesia in a dose-dependent manner in diabetic *ob/ob* mice.⁴ *In vivo* silencing of α_{1H} in sensory neurons alleviates hyperalgesia in rat models with

streptozotocin (STZ)-induced DPN.⁵ Therefore, the modulation of T-type calcium channels could serve as an important target in the treatment of painful PDN symptoms. This report describes the development of potent α_{1H} channel inhibitors for the treatment of diabetic neuropathic pain (DNP).

T-type calcium channels are classified into three types, α_{1G} , α_{1H} , and α_{1I} , based on molecular cloning of the α_1 subunit. All three of the cloned T-type calcium channels are present in the spinal dorsal horn, with the α_{1G} and α_{1H} subtypes being most prominent in lamina I.⁶ Studies of *in situ* hybridization and reverse-transcription polymerase chain reaction (PCR) have shown that α_{1H} is most highly expressed in DRG neurons, while α_{1G} and α_{1I} are present at lower levels.⁷ T-type calcium channels are important therapeutic targets in pain treatments. Intrathecal administration of α_{1H} -specific, but not α_{1G} - or α_{1I} -specific, antisense oligonucleotides has led to anti-nociceptive, and anti-allodynia effects in acute and neuropathic pain models.⁸ We previously reported that aryl (1,5-disubstituted-pyrazol-3-yl)methyl sulfonamides were T-type calcium channel inhibitors.⁹ The most active candidate, 3-fluorophenyl((1-phenyl-5-isopropyl)pyrazol-3-yl)sulfonamide, showed good T-type calcium channel-blocking effects and good pharmacokinetic properties, with the exception of microsomal stability, as well as potent anti-neuropathic pain effects.

In a continuing effort to develop metabolically stable, potent α_{1H} channel blockers, we have designed and synthesized a novel series of fused-benzosulfonamides substituted at the nitrogen with a (1,5-disubstituted pyrazol-3-yl)methyl moiety. The substituent R¹ and R² on pyrazole ring have designed hydrophobic

* Corresponding author at: Center for Neuro-Medicine, Brain Science Institute, Korea Institutes of Science and Technology (KIST), Seoul 02792, Republic of Korea.

E-mail address: gsnam@kist.re.kr (G. Nam).

^c These authors made comparable contributions to this research.

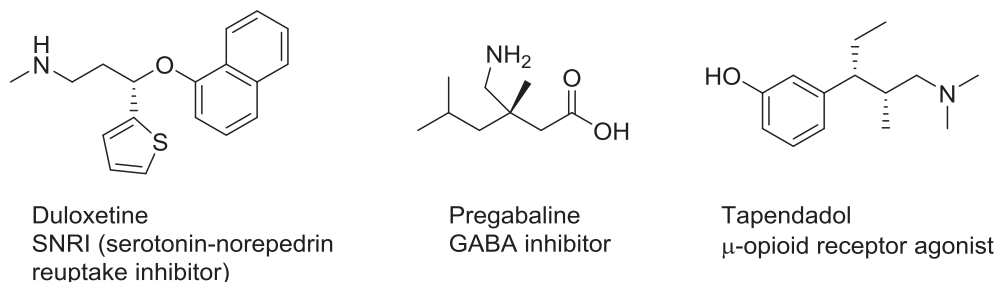


Fig. 1. FDA-approved PDN drugs.

group such as phenyl, substituted phenyl and *t*-butyl group, and bulky aliphatic groups such as *i*-butyl and *t*-butyl groups. We describe herein the synthesis of 2*N*-(pyrazol-3-yl)methylbenzo[*d*]isothiazole 1,1-dioxide derivatives and evaluate their α_{1H} T-type channel inhibitory activity, structure–activity relationships (SARs), pharmacokinetic properties, and *in vivo* efficacy against STZ-induced DNP in a rat model. The chemical structure of previous candidate **A** and designed molecule in the current study are shown in Fig. 2.

2. Chemistry

Previously reported candidate compound **A** exhibited strong T-type calcium channel inhibition and anti-neuropathic pain effects with low metabolic stability (13.88% HLM).⁹

Generally, chemical structural modification strategies have applied to increase the metabolic stability of compounds.¹⁰

To overcome their inherently low metabolic stability, a methyl group was introduced to previous candidate aryl(1,5-disubstituted-pyrazol-3-yl)methyl sulfonamides, and a fused methylene-bridged ring was prepared between the phenyl and sulfonamide groups, as in benzo[*d*]isothiazole-3(2*H*)-one-1,1-dioxide. Methyl groups were added to the open ring skeletons of compounds **4** and **5** at the nitrogen of the sulfonamide and the 4-position of pyrazole, respectively, as outlined in Scheme 1. *N*-Methylated sulfonamide **4** was prepared by sulfonylation of *N*-methylamine derivatives **3a** with phenyl sulfonyl chloride. The ester derivative **1a** was reduced to an alcohol and subjected to azidation via the Mitsunobu reaction (Merck method),¹¹ to give the azide compound **2a**. The azide group of compound **2a** was reduced to an amine, followed by monomethylation using triphenyl phosphine and methyl iodide to give (5-isopropyl-1-phenyl)-3-pyrazolylmethyl-*N*-methylamine **3a**. Also, the tri-substituted pyrazolyl(phenyl) sulfonamide **5**, possessing a methyl group at the C-4 position of the pyrazole ring, was prepared by the coupling of (5-isopropyl-4-methyl-1-phenyl)-pyrazol-3-methyl amine **3b** with phenyl sulfonyl chloride. The (pyrazol-3-yl)methylamine **3b** was prepared from (1-phenyl-5-isopropyl)pyrazol-3-acetate **1b** by reduction of the ester using DIBAL-H, followed by its transformation into hydroxime and subsequent reduction with lithium aluminum hydride in three steps.

Compounds **9–19**, fused-benzenesulfonamide ring analogues linked with an *N*-methylene group, were synthesized by the route shown in Scheme 2. Reduction of pyrazol-3-yl ester **1** by LAH, followed by bromination of the corresponding alcohol using PBr_3/PPh_3 , afforded 3-bromomethylpyrazole **6a–h**. Nucleophilic substitution of **6** with 2,3-dihydrobenzo[*d*]isothiazole 1,1-dioxide **8**, prepared by the reduction of commercially available benzo[*d*]isothiazole-3(2*H*)-one 1,1-dioxide **7**, gave 2*N*-(pyrazol-5-yl)methylbenzo[*d*]isothiazole 1,1-dioxide derivatives **9–19** as fused-ring skeletons.

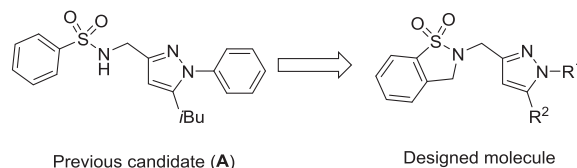


Fig. 2. Structure of designed molecules.

3. Results and discussion

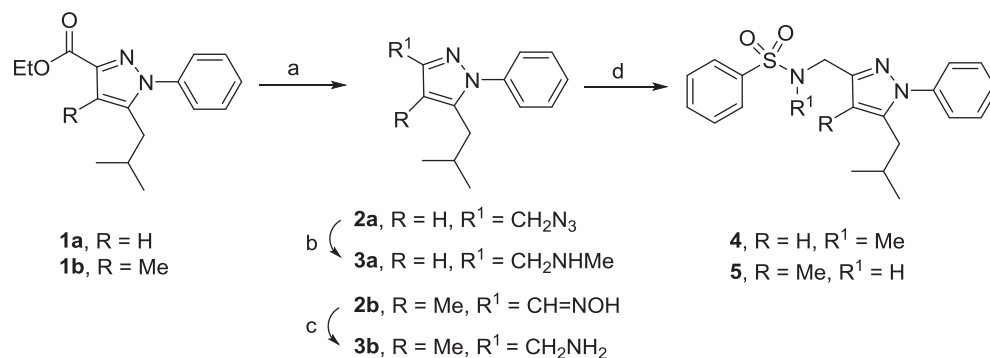
The *in vitro* calcium channel inhibitory activities of all of the synthesized compounds were screened using a high throughput screening (HTS) FDSS6000 method against $Ca_v3.2$ (α_{1H}) calcium channels. IC_{50} values were determined for compounds showing more than 60% inhibition.¹² The results are summarized in Table 1.

The synthesized compounds displayed a broad range of inhibition (9.86–75.51%) of α_{1H} T-type calcium channels. The activity of fused-benzene sulfonamides **9–19** depended on the nature of the R^1 and R^2 substituents on the pyrazole ring. The introduction of hydrophobic groups, such as phenyl (**9**, 75.51%) and 4-fluorophenyl (**10**, 71.57%) groups on R^1 , and an isopropyl group on R^2 , resulted in high degrees of inhibition. The introduction of sterically hindered aliphatic alkyl substituents, such as *t*-butyl (**13–17**) and *i*-propyl (**18**, **19**) groups on R^1 and aromatic substituents, such as phenyl, monosubstituted phenyl and cyclohexyl groups, as well as piperidine derivatives containing phenyl groups on R^2 , resulted in low degrees of inhibitory activity (9.86–23.06%). Compounds having both alkyl substituents R^1 and R^2 displayed moderate activity levels (**17**, 68.04%). For open-type benzenesulfonamides (**A**, **4** and **5**, $R^1 = Ph$, $R^2 = i$ -propyl), the substituent effects were similar to those of fused-benzosulfonamide derivatives. This result demonstrates that R^1 substituents having aromatic groups are more potent than aliphatic groups for the inhibition of α_{1H} T-type calcium channels.

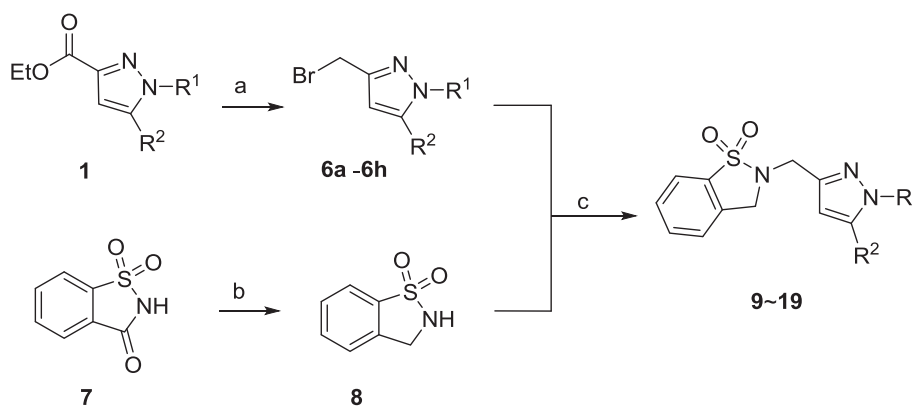
The HLM (human liver microsomal) stabilities of selected compounds were evaluated and listed in Table 1. The methyl group introduced compound **4** and **5**, ring cyclized compound **9** of compound **A** decreased HLM stability than compound **A**. Compound **10** ($R^1 = 4$ -FPh, $R^2 = i$ -Pro) and compound **17** ($R^1 = t$ -But, $R^2 = i$ -Pro) significantly increased HLM stability.

To determine the pharmaceutical suitability of the synthesized materials, compounds **A** ($IC_{50} = 5.80 \pm 0.61$), **5** ($IC_{50} = 4.30 \pm 0.84$), **9** ($IC_{50} = 2.52 \pm 0.83$), **10** ($IC_{50} = 2.32 \pm 0.73$) and **17** ($IC_{50} = 3.69 \pm 0.60$) were evaluated for their inhibitory activity against human cytochrome P450 and the hERG channel (Table 2).

Compounds **9**, **10** and **17** exhibited low inhibitory potency against CYP2D6, which is known to induce the metabolism of several central nervous system and cardiovascular system-related drugs.¹³ All of the tested compounds displayed moderate levels of inhibition of CYP3A4. Among them, compounds **10** ($R^1 = 4$ -FPh, $R^2 = i$ -propyl), and **17** ($R^1 = t$ -butyl, $R^2 = i$ -propyl), both bearing



Scheme 1. Reagents and conditions: (a) i) 1.0 M LAH in ether, THF, 0 °C to rt, 95%, ii) (PhO)₂PON₃, DBU, THF, for **1a**; or i) DIBAL-H, DCM, -78 °C, yield 73%, ii) hydroxylamine-HCl, TEA, DCM, rt, yield 50–90% for **1b**; b) PPh₃, CH₃I, THF; c) 1.0 M LAH, THF, 0 °C to rt, 76–95%; (d) PhSO₂Cl, K₂CO₃, DCM/DMF, rt, 30–61%.



Scheme 2. Reagents and conditions: (a) i) 1.0 M LAH in ether, THF, 0 °C to rt, 95%; ii) PBr₃, PPh₃, DCM, 0 °C, 27–64%; (b) 1.0 M LAH, THF, rt, 38%; (c) K₂CO₃, DCM/DMF, rt, 30–61%.

fused-benzenesulfonamides, showed relatively low inhibition of all of the tested CYP enzymes. Thus, these two compounds would not be expected to be disadvantaged by drug-drug interactions. Compounds **10** and **17** showed high microsomal stability and low hERG inhibition. Contrary to expectations, a methyl group was introduced in *N*-position of sulfonamide (compound **4**) and attached at C4 position on pyrazole ring (compound **5**) displayed lower stabilities than that of compound **A**, which lacks a methyl group.

Compounds **9** and **10** were the most potent inhibitors of T-type α_{1H} calcium channels, having IC₅₀ values (half maximum inhibition concentrations) of 2.52 ± 0.83 and 2.32 ± 0.73 against α_{1H} , respectively, and also showing favorable pharmacological properties, including low inhibition potency against CYP450 and hERG channels. Compound **10** showed high human liver microsomal stability although the compound **9** having low HLM stability. These results suggest that, relative to unsubstituted phenyl substituents, the 4-fluorophenyl group at the R¹ substituent of the pyrazole ring in fused-benzenesulfonamide skeleton plays an important role in determining metabolic stability.

Finally, we evaluated candidate compound **10** (R¹ = 4-FPh, R² = *i*-butyl) for DNP alleviation *in vivo*. The pharmacokinetic data of compound **10** are summarized in Table 3.

The efficacy of the selected compounds for alleviating DNP was determined by behavioral tests of reduced hyperalgesia in an STZ-induced DNP rat model.⁵ The anti-algectic effect of compound **10** on DNP was examined and compared to that of gabapentin in a single oral treatment of 100 mg/kg in each of five or six DNP rats. The results are presented in Fig. 3.

The efficacy of compound **10** against DNP pain was highest within 1 h after administration in both mechanical allodynia with

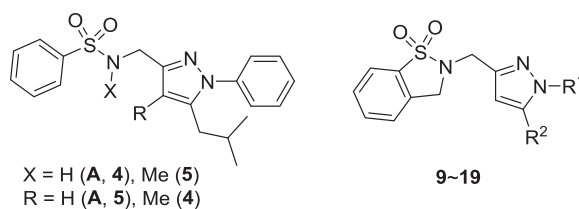
heat hypersensitivity tests. However, the efficacy of the anti-algectic effect decreased at 3 h (Fig. 2). In contrast, gabapentin did not show any pain-reducing activity 1 h after treatment. Instead, the activity increased after 3 h and remained constant up to 5 h after the initial mechanical allodynia. Against heat allodynia, gabapentin also exhibited pain-reducing activity within 1 h, which persisted until 5 h after administration. Therefore, the anti-algectic effect of compound **10** on DNP was faster-acting than that of gabapentin, but the duration of activity was relatively short. Therefore, to investigate any possible synergic effects of gabapentin and compound **10**, compound **10** (50 mg/kg) and gabapentin (50 mg/kg) were co-administrated orally, and their combined anti-nociceptive effects on DNP were compared against a single administration of each (Fig. 4).

Single low doses (50 mg/kg) of compound **10** did not exhibit any inhibition of cold or mechanical allodynia at 1 h or 5 h, although high doses (100 mg/kg) showed excellent anti-allodynia effects after 1 h of administration. High doses of gabapentin exhibited similar effects from 1 h after treatment. Co-administration of compound **10** (50 mg/kg) with gabapentin (50 mg/kg) increased the degree of pain alleviation more than the sum of individual administrations, particularly at 3 h after treatment. The maximum synergic effect against mechanical allodynia was observed at 3 h, with a 3-fold increase of activity relative to that of a single dose of gabapentin.

4. Conclusions

To develop T-type calcium channel blockers having greater microsomal stability, a novel series of 2*N*-(pyrazol-5-yl)methyl-

Table 1
Percent inhibition and IC₅₀ values against T-type (α_{1H}) calcium channels, and human liver microsomal stabilities of substituted *N*-pyrazolylmethyl sulfoamides and their fused-benzenesulfonamide derivatives.



Compd.	R ₁	R ₂	α_{1H}		HLM ^d Stability Remaining%
			% inhibition (10 μ M) ^a	IC ₅₀ (μ M) ^b	
A			63.86	5.80 \pm 0.61	13.88
4			54.24	ND ^c	1.46
5			72.00	4.30 \pm 0.84	0.26
9	Ph	<i>i</i> -propyl	75.51	2.52 \pm 0.83	4.69
10	4-FPh	<i>i</i> -Propyl	71.57	2.32 \pm 0.73	101.55
11	1,6-Cl ₂ -Ph	<i>i</i> -Propyl	29.51	ND ^c	ND ^c
12	<i>t</i> -Butyl	Ph	18.66	ND ^c	ND ^c
13	<i>t</i> -Butyl	4-FPh	23.06	ND ^c	ND ^c
14	<i>t</i> -Butyl	4-CF ₃ Ph	20.79	ND ^c	ND ^c
15	<i>t</i> -Butyl	4-piperidylPh	16.34	ND ^c	ND ^c
16	<i>t</i> -Butyl	4-cyclohexylPh	9.86	ND ^c	ND ^c
17	<i>t</i> -Butyl	<i>i</i> -propyl	68.04	3.69 \pm 0.60	102.96
18	<i>i</i> -Propyl	Ph	22.05	ND ^c	ND ^c
19	<i>i</i> -Propyl	4-FPh	16.48	ND ^c	ND ^c

^a % inhibition was obtained using a FDSS6000 assay.

^b IC₅₀ values (\pm SD) were obtained from a dose-response curve using a whole cell patch clamp.

^c Not determined.

^d HLM, human liver microsomal.

Table 2
In vitro activity of selected compounds against cytochrome P450 and hERG channels.

Compd.	% control of CYP-450 (10 μ M) ^a				hERG channel
	1A2 ^b	2D6 ^c	2C9 ^d	3A4 ^e	IC ₅₀ (μ M) ^f
5	NT ^g	45.23	45.23	38.69	NT ^g
9	NT ^g	86.63	14.17	47.17	NT ^g
10	109.59	90.63	103.11	45.67	14.70 \pm 3.30
17	123.41	78.83	90.65	52.13	19.30 \pm 4.71

^a Values represent the remaining % activities and the mean \pm SD from triplicate experiments.

^b α -Naphthoflavone.

^c Quinidine.

^d Sulfaphenazol.

^e Ketoconazole.

^f IC₅₀ values (\pm SD) were obtained from a dose-response curve using a patch clamp.

^g Not tested.

benzo[*d*]thiazole-1,1-dioxide derivatives, containing a fused-benz-sulfonamide moiety, were designed and synthesized using known methods. SARs of the synthesized compounds against the α_{1H} T-type calcium channel, and *in vivo* pain-alleviating efficacy against DNP, are reported. The presence of the fused-benz-sulfonamide increased microsomal stability, although introducing a methyl group at the amine or at the pyrazole ring decreased microsomal stability.

The nature of the substituent at the N1 and C5 positions of pyrazole, R¹ and R² respectively, plays a crucial role in determining the *in vitro* α_{1H} T-type calcium channel inhibitory activity. Compounds having hydrophobic R¹ (Ph and 4-FPh) and aliphatic R² (*i*-propyl) substituents at the pyrazole moiety showed high inhibitory

activities, while substitution with aliphatic R¹ (*t*-butyl) and aromatic R² groups including bulky-substituents resulted in low potency. Pyrazole compounds with both aliphatic R¹ and R² substituents also showed high inhibitory potency against α_{1H} T-type calcium channels.

Compound **10** exhibited the highest pain-alleviating effect in STZ-induced DNP rat models, as well as the most favorable pharmacokinetic properties. Compound **10** exhibited a rapid onset of activity against mechanical allodynia. Furthermore, co-administration of compound **10** with gabapentin at low doses displayed a positive synergic effect in an *in vivo* DNP model. These data point toward the importance of α_{1H} T-type calcium channels in the treatment of DNP.

Table 3

Pharmacokinetic parameters following intravenous (n = 5) and oral (n = 4) administration (10 mg/kg) of **10** to male rats.

	10 (mean ± SD ^a)	
	iv	Oral
AUC _{0–∞} (μg min/ml)	178.68 ± 34.54	16.45 ± 9.02
AUC _{last} (μg min/ml)	157.86 ± 27.88	14.60 ± 6.86
Terminal half-life (min)	176.12 ± 85.31	117.38 ± 63.70
C _{max} (μg/ml)	–	0.10 ± 0.06
T _{max} (min)	–	150 (120–240) ^b
CL (ml/min/kg)	57.70 ± 11.38	–
MRT (min)	102.29 ± 55.73	–
Brain-to-plasma ratio (B/P) at 2 h	1.28	0.13
F (%)	9.2	–

Abbreviations: AUC_{0–∞}, total area under the plasma concentration–time curve from time zero to infinity; AUC_{last}, total area under the plasma concentration–time curve from time zero to the previous time; C_{max}, peak plasma concentration; T_{max}, time to reach C_{max}; CL, time-averaged total body clearance; MRT, mean residence time; F, bioavailability.

^a SD: standard deviation.

^b Median (range) for T_{max}.

5. Experimental section

5.1. Chemistry

5.1.1. General

Commercially available solvents and reagents were used without additional purification. The reaction progress was monitored

on analytical thin-layer chromatography (Merck, silica gel 60F254) with a UV lamp at 254 and 365 nm. Column chromatography was used by silica gel (Merck, 230–400 mesh). ¹H and ¹³C NMR spectra were recorded on a Bruker Advance 300 or 400 MHz spectrometer. A Q-TOF SYNAPT G2 Mass spectrometry (Waters MS Technologies, Manchester, UK) was used for measuring compound mass.

5.1.2. Ethyl(4-ethyl-5-isobutyl-1-phenyl-1H-pyrazole)-3-carboxylate (**1a**)

Phenyl hydrazine (911 μL, 9.27 mmol) was added to a solution of ethyl (Z)-(3-ethyl-2-hydroxy-6-methyl-4-oxohept-2-eno)ate (1.86 g, 9.27 mmol) in ethanol. After stirring for 1 h at room temperature, 1N HCl was added to the solution and stirred for overnight. The reaction mixture was extracted with dichloromethane. The organic layer was dried over magnesium sulfate, filtered in vacuo, and purified by column chromatography (hexane:EtOAc = 10:1 then 1:1) to afford 1.95 g (77.4%) of the title compound. ¹H NMR (400 MHz, CDCl₃) δ 7.48–7.40 (m, 5H), 6.76 (s, 1H), 4.41 (q, J = 7.1 Hz, 2H), 2.51 (d, J = 7.2 Hz, 2H), 1.87–1.79 (m, 1H), 1.40 (t, J = 7.12 Hz, 3H), 0.86 (d, J = 6.6 Hz, 6H).

5.1.3. Ethyl (5-isobutyl-4-methyl-1-phenyl-1H-pyrazole)-3-carboxylate (**1b**)

Ethyl (Z)-2-hydroxy-3,6-dimethyl-4-oxohept-2-enoate (1.94 g, 9.06 mmol) was reacted with phenyl hydrazine (890 μL,

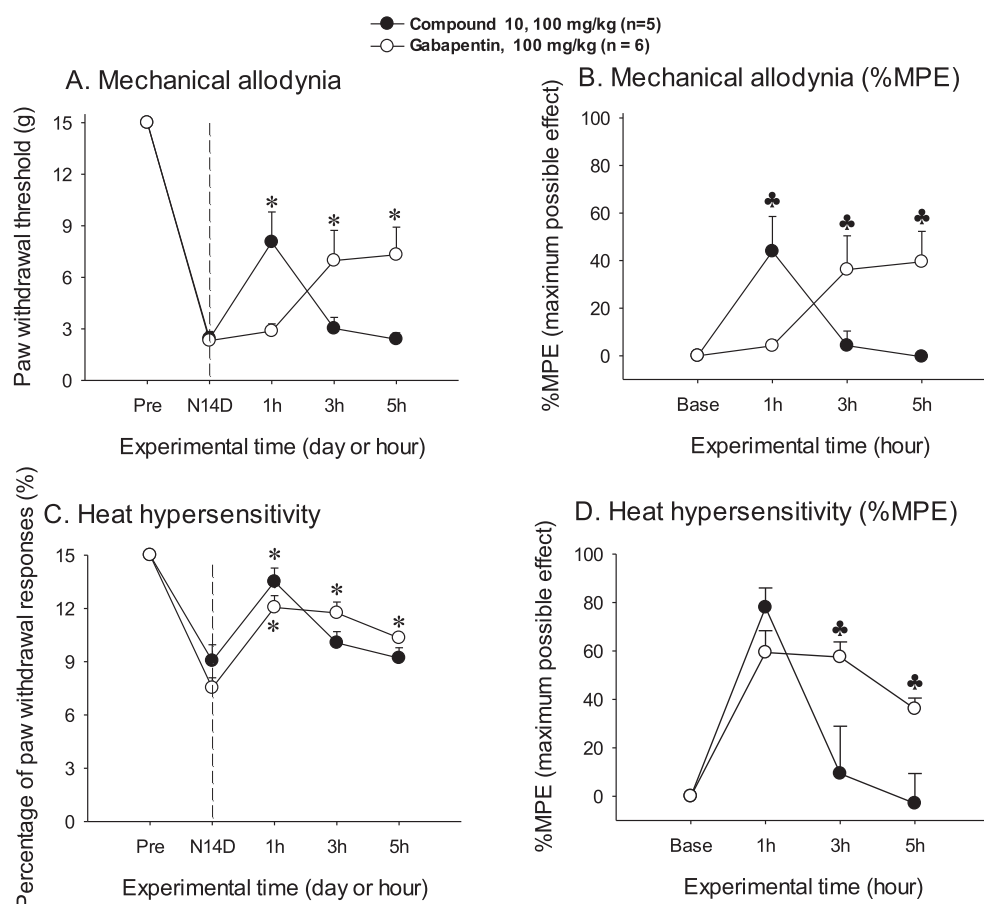


Fig. 3. Effects on mechanical allodynia (A and B) and heat hypersensitivity (C and D) of oral administration of gabapentin (○, 100 mg/kg, n = 6) and compound **10** (●, 100 mg/kg, n = 5) to neuropathic pain-induced rats. Experimental time is expressed as D (days) after neuropathic injury (N) and h (hours) after gabapentin or compound **10** administration. *P < 0.05 (gabapentin), †P < 0.05 (compound **10**) vs. pre-administration value (paired t-test), ▲P < 0.05 gabapentin vs. compound **10** unpaired t-test.

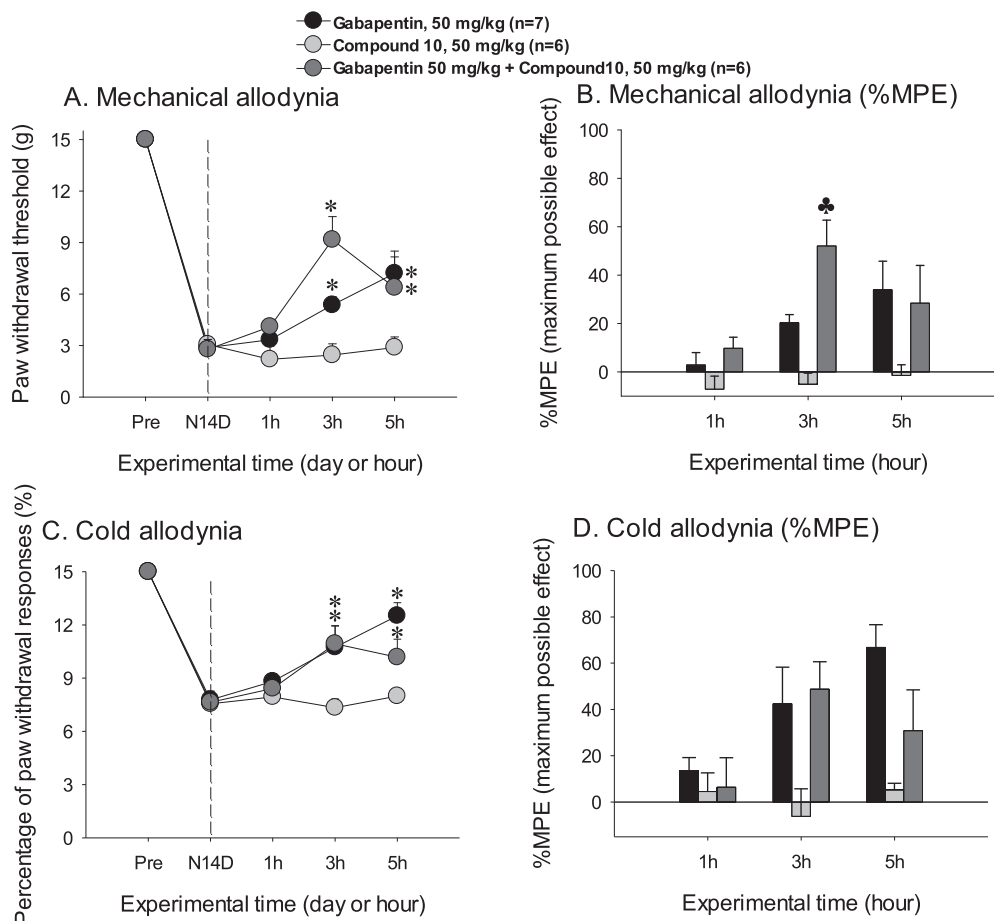


Fig. 4. Effects on mechanical allodynia (A and B) and heat hypersensitivity (C and D) of oral administration of gabapentin (●, 50 mg/kg, $n = 7$), compound **10** (○, 50 mg/kg, $n = 6$) and gabapentin + compound **10** (⊙, 50 mg/kg, $n = 6$) to neuropathic pain-induced rats. Experimental time is expressed as D (days) after neuropathic injury (N) and h (hours) after gabapentin, compound **10** and gabapentin + compound **10** administration. * $P < 0.05$ (gabapentin, compound **10** and gabapentin + compound **10**) vs. pre-administration value (paired t -test), ** $P < 0.05$ Co-treatment of gabapentin and compound **10** vs. gabapentin or compound **10** (unpaired t -test).

9.06 mmol) following same procedure of **1a**. Final reaction mixture was purified by column chromatography (hexane:EtOAc = 11: 1 then 6: 1) to afford the title compound (540 mg). $^1\text{H NMR}$ (400 MHz, CDCl_3) δ 7.46–7.38 (m, 5H), 4.42 (q, $J = 7.1$ Hz, 2H), 2.51 (d, $J = 7.5$ Hz, 2H), 2.30 (s, 3H), 1.60–1.52 (m, 1H), 1.41 (t, $J = 7.1$ Hz, 3H), 0.74 (d, $J = 6.7$ Hz, 6H).

5.1.4. 3-Azidomethyl-5-isobutyl-1-phenyl-1H-pyrazole (**2a**)

Dried ethyl 4-ethyl-5-isobutyl-1-phenyl-1H-pyrazole-3-carboxylate (1.76 mg, 6.47 mmol) was dissolved in diethyl ether (2.0 mL) and dichloromethane (2.0 mL), and lithium aluminum hydride (1 M in hexane, 14.2 mL) was added at -0°C to the solution. After the temperature of the reaction mixture was elevated to room temperature, it was added with water and filtered out. The reaction mixture was extracted with dichloromethane. The organic layer was concentrated to give alcohol compound (1.48 g, 99.2%). Diphenyl phosphoryl azide (260 μL , 1.20 mmol) and 1,8-diazabicyclo[5.4.0]undec-7-ene (179 μL , 1.20 mmol) was added to the reduced compound (231 mg, 1.00 mmol) in THF. After stirring 16 h, the reaction mixture was diluted with toluene, and washed with 5% HCl. The organic layer was dried over magnesium sulfate, and solvent was removed by rotary evaporator to afford the title compound (255 mg, 100%). $^1\text{H NMR}$ (400 MHz, CDCl_3) δ 7.48–7.38 (m, 5H), 6.23 (s, 1H), 4.39 (s, 2H), 2.52 (d, $J = 7.3$ Hz, 2H), 1.85–1.78 (m, 1H), 0.87 (d, $J = 6.6$ Hz, 6H).

5.1.5. 3-(Hydroxyamino)methyl-5-isobutyl-4-methyl-1-phenylpyrazole (**2b**)

Diisobutylaluminum hydride (1.0 M hexane, 2.88 mL) was added to a solution of compound **1b** (273 mg, 0.95 mmol) in dichloromethane (1.0 mL) at -78°C , and stirred for 1 h. The reaction mixture was extracted with dichloromethane. The organic fraction was dried over MgSO_4 , and purified by column chromatography to give the corresponding aldehyde compound. This aldehyde compound (194 mg, 0.80 mmol) was added to a solution of hydroxylamine hydrochloride (61.2 mg, 0.88 mmol) and triethyl amine (123 μL , 0.80 mmol) in dichloromethane, and stirred for 4 h. The reaction mixture was extracted with dichloromethane and washed with brine. The organic layer was dried over MgSO_4 , solvent was concentrated with reduced pressure to afford the title compound (196 mg, 95%). $^1\text{H NMR}$ (400 MHz, CDCl_3) δ 8.29 (s, 1H), 7.47–7.37 (m, 5H), 2.53 (d, $J = 7.4$ Hz, 2H), 2.21 (s, 3H), 1.68–1.60 (m, 1H), 0.74 (d, $J = 6.7$ Hz, 6H).

5.1.6. 5-Isobutyl-1-phenyl-1H-pyrazol-3-yl)methanamine (**3a**)

Polymer supported triphenyl phosphine (940 mg, 1.50 mmol) was dissolved in THF (17 mL), and compound **2a** (180 mg, 0.75 mmol) was added to the triphenyl phosphine solution, and stirred for 4 h. Methyl iodide (141 μL , 2.26 mmol) was added to the reaction mixture and reacted for overnight. The solid resin was filtered and washed with dichloromethane, and the filtered

resin was pour into MeOH. Then KOH (2% MeOH, 28 mL) was added to the reaction mixture and stirred for 4 h at 65 °C. The solid was filtered off and residual solution was extracted with dichloromethane, dried over Na₂SO₄ and solvent was removed to give compound **3a** (98.5 mg, 53.8%). ¹H NMR (400 MHz, CDCl₃) δ 7.47–7.38 (m, 5H), 6.17 (s, 1H), 3.80 (s, 2H), 2.51 (s, 3H), 2.50 (d, *J* = 6.2 Hz, 2H), 1.88–1.79 (m, 1H), 0.85 (d, *J* = 6.2 Hz, 6H).

5.1.7. 5-Isobutyl-4-methyl-1-phenyl-1H-pyrazol-3-yl)methanamine (3b)

After dissolving the compound **2b** (195 mg, 0.76 mmol) in ether (1.0 mL) and THF (2.0 mL), lithium aluminium hydride (1 M in ether 1.67 mmol) was added, and stirred for 30 min at 0 °C and 4 h at room temperature. Sodium sulfate hydrate was added carefully to the reaction mixture at 0 °C. The reaction mixture was filtered through Celite and Na₂SO₄ and the mixture was concentrated over reduced pressure to give amine product **3b** (178 mg, 96.5%). ¹H NMR (400 MHz, CDCl₃) δ 7.46–7.34 (m, 5H), 3.87 (s, 2H), 2.51 (d, *J* = 7.4 Hz, 2H), 2.04 (s, 3H), 1.88–1.55 (m, 1H), 0.75 (d, *J* = 6.6 Hz, 6H).

5.1.8. N-Methyl[(5-isobutyl-1-phenyl-1H-pyrazol-3-yl)methyl]benzenesulfonamide (4)

Triethylamine (80.0 μL, 0.43 mmol) was added to a solution of **3a** (95.3 mg, 0.39 mmol) in dichloromethane (3.0 mL) at 0 °C and stirred for 5 min. Benzenesulfonyl chloride (52.6 μL, 0.41 mmol) was added to the reaction mixture and stirred for 1 h at room temperature. Then, water and a saturated NaHCO₃ solution were added to the solution before extraction with dichloromethane. The organic layer was dried over magnesium sulfate, concentrated *in vacuo*, and purified by column chromatography (hexane: EtOAc = 3:1) to afford the title compound (78.8 mg, 52.5%). ¹H NMR (400 MHz, CDCl₃) δ 7.85–7.83 (m, 2H), 7.60–7.51 (m, 3H), 7.48–7.42 (m, 2H), 7.40–7.32 (m, 3H), 6.18 (s, 1H), 4.26 (s, 2H), 2.72 (s, 2H), 2.48 (d, *J* = 7.2 Hz, 2H), 1.83–1.76 (m, 1H), 0.85 (d, *J* = 6.6 Hz, 6H); ¹³C NMR (100 MHz, CDCl₃) δ 147.7, 144.6, 139.7, 137.4, 132.6, 129.1, 129.0, 128.0, 127.5, 125.6, 105.5, 47.9, 35.2, 34.6, 28.3, 22.4.

5.1.9. N-Methyl[(5-Isobutyl-1-phenyl-1H-pyrazol-3-yl)methyl]benzenesulfonamide (5)

Compound **3b** (55.7 mg, 0.229 mmol) was reacted with benzenesulfonyl chloride (30.7 μL, 0.24 mmol) following same procedure of compound **4** to give target compound **5** (77.1 mg, 87.8%). ¹H NMR (400 MHz, CDCl₃) δ 7.88–7.84 (m, 2H), 7.53–7.50 (m, 3H), 7.46–7.35 (m, 5H), 7.24–7.22 (m, 2H), 5.53 (bs, 1H), 4.12 (d, *J* = 5.7 Hz, 2H), 2.44 (d, *J* = 7.4 Hz, 2H), 1.94 (s, 3H), 1.58–1.50 (m, 1H), 0.69 (d, *J* = 6.6 Hz, 6H); ¹³C NMR (100 MHz, CDCl₃) δ 147.8, 141.1, 140.0, 139.7, 132.5, 129.1, 128.9, 128.0, 127.1, 125.7, 113.1, 39.7, 33.2, 28.4, 22.2, 8.08.

5.1.10. 3-Bromomethyl-5-isopropyl-1-phenyl-1H-pyrazole (6)

General method. Phosphorous tribromide (531 μL, 5.65 mmol) was added to a solution of (5-R²-3-hydroxymethyl-1-R¹)pyrazole (5.14 mmol) in dichloromethane (3.0 mL) at 0 °C, and stirred for 3 h at room temperature. Subsequently, the reaction mixture was extracted with dichloromethane and washed with brine. The organic layer was dried over magnesium sulfate and concentrated *in vacuo*, and purified by column chromatography (hexane: EtOAc = 1:1) to afford the title compound.

5.1.11. 3-Bromomethyl-5-isopropyl-1-phenyl-1H-pyrazole (6a)

Yield 85%; ¹H NMR (300 MHz, CDCl₃) δ 7.54–7.42 (m, 5H), 6.32 (s, 1H), 4.57 (s, 2H), 2.54 (d, *J* = 7.2 Hz, 2H), 1.91–1.82 (m, 1H), 0.91 (d, *J* = 6.6 Hz, 6H).

5.1.12. 3-Bromomethyl-5-isopropyl-1-(p-fluorophenyl)-1H-pyrazole (6b)

Yield 83%; ¹H NMR (300 MHz, CDCl₃) δ 7.43–7.31 (m, 2H), 7.22–7.17 (m, 2H), 6.25 (s, 1H), 4.76 (d, *J* = 5.9 Hz, 2H), 2.51 (d, *J* = 7.2 Hz), 1.98 (t, *J* = 5.9 Hz, 1H), 1.92–1.79 (m, 1H), 0.91 (d, *J* = 6.6 Hz, 6H).

5.1.13. 3-Bromomethyl-5-isopropyl-1-(2,6-dichlorophenyl)-1H-pyrazole (6c)

Yield 99%; ¹H NMR (300 MHz, CDCl₃) δ 7.52–7.38 (m, 3H), 6.28 (s, 1H), 4.79 (d, *J* = 6.1 Hz, 2H), 2.29 (d, *J* = 7.3 Hz, 2H), 1.98–1.85 (m, 2H), 0.95 (d, *J* = 6.6 Hz, 6H).

5.1.14. 3-Bromomethyl-1-t-butyl-5-phenyl-1H-pyrazole (6d)

Yield 19%; ¹H NMR (300 MHz, CDCl₃) δ 7.45–7.37 (m, 5H), 6.24 (s, 1H), 4.57 (s, 2H), 1.47 (s, 9H).

5.1.15. 3-Bromomethyl-1-t-butyl-5-(p-fluorophenyl)-1H-pyrazole (6e)

Yield 98%; ¹H NMR (300 MHz, CDCl₃) δ 7.37–7.33 (m, 2H), 7.12 (t, *J* = 8.6 Hz, 2H), 4.73 (d, *J* = 5.7 Hz, 2H), 2.03 (t, *J* = 5.7 Hz, 1H), 1.48 (s, 9H).

5.1.16. 3-Bromomethyl-1-t-butyl-5-(p-trifluorophenyl)-1H-pyrazole (6f)

¹H NMR (300 MHz, CDCl₃) δ 7.70 (d, *J* = 8.0 Hz, 2H), 7.53 (d, *J* = 8.0 Hz, 2H), 6.25 (s, 1H), 4.56 (s, 2H), 1.48 (s, 9H).

5.1.17. 3-Bromomethyl-1-t-butyl-5-isopropyl-1H-pyrazole (6g)

Yield 41%; ¹H NMR (300 MHz, CDCl₃) δ 6.18 (s, 1H), 4.51 (s, 2H), 2.67 (d, *J* = 6.7 Hz, 2H), 2.10–1.95 (m, 1H), 1.65 (s, 9H), 1.03 (d, *J* = 6.6 Hz, 6H).

5.1.18. 3-Bromomethyl-1-isopropyl-5-phenyl-1H-pyrazole (6h)

Yield 99%; ¹H NMR (300 MHz, CDCl₃) δ 7.48–7.39 (m, 5H), 6.29 (s, 1H), 4.76 (d, *J* = 6.0 Hz, 2H), 3.92 (d, *J* = 7.6 Hz, 2H), 2.24–2.17 (m, 1H), 1.95 (t, *J* = 6.0 Hz, 1H), 0.79 (d, *J* = 6.8 Hz, 6H).

5.1.19. 1,2-Bezeneisothiazolin-1,1-dioxide (8)

Lithium aluminium hydride 1 M in ether (4.09 mL) was added slowly at 0 °C to a solution of *o*-sulfobenzimide (**7**, 554 mg, 3.02 mmol) in THF (8.0 mL), and stirred for 48 min. Subsequently, sodium sulfate hydrate was added to the solution and filtered through Celite. The organic layer was concentrated in reduced pressure to afford the title compound (182 mg, 35.6%); ¹H NMR (400 MHz, CDCl₃) δ 7.85 (d, *J* = 7.7, 1H), 7.67 (dt, *J* = 7.5, 1.2 Hz, 1H), 7.58 (t, *J* = 7.4 Hz, 1H), 7.44 (d, *J* = 7.6 Hz, 1H), 4.74 (br, 1H), 4.59 (s, 2H).

5.2. General procedure for the synthesis of compound 9–19

Potassium carbonate was dissolved in DMF, and 1,2-bezeneisothiazolin-1,1-dioxide (**8**) (1 equiv.) in dichloromethane was added to the reaction solution, and stirred for overnight. Then, the reaction mixture was filtered through Celite, and washed with 1 N HCl and saturated sodium hydrogen carbonate solution. Residual solution was dried over magnesium sulfate, and concentrated *in vacuo*, and purified by column chromatography to afford the title compound.

5.2.1. 2-[(5-isopropyl-1-phenyl-1H-pyrazol-3-yl)methyl]-2,3-dihydrobenzo[d]isothiazole 1,1-dioxide (9)

Yield; 85.5%; ¹H NMR (400 MHz, CDCl₃) δ 7.81–7.79 (m, 2H), 7.58–7.33 (m, 8H), 6.36 (s, 2H), 4.54 (s, 2H), 4.39 (s, 2H), 2.50 (d, *J* = 7.0 Hz, 2H), 1.84–1.77 (m, 1H), 0.84 (d, *J* = 6.6 Hz, 6H); ¹³C NMR (100 MHz, CDCl₃) δ 147.2, 144.7, 139.7, 135.1, 134.0, 132.6,

129.2, 129.0, 125.7, 124.6, 121.3, 106.0, 50.0, 41.3, 35.2, 28.3, 22.4. HRMS [ESI⁺] *m/z* calcd for C₂₁H₂₃N₃O₂S [M + H]⁺: 382.1511, found: 382.1600.

5.2.2. 2-[(1-(4-fluorophenyl)-5-isobutyl-1H-pyrazol-3-yl)methyl]-2,3-dihydrobenzo[d]isothiazole 1,1-dioxide (**10**)

Yield 79%; ¹H NMR (300 MHz, CDCl₃) δ 7.83–7.49 (m, 3H), 7.41–7.34 (m, 3H), 7.20–7.14 (m, 2H), 6.35 (s, 1H), 4.52 (s, 2H), 4.39 (s, 2H), 2.46 (d, *J* = 7.2 Hz, 2H), 1.87–1.73 (m, 1H), 0.84 (d, *J* = 6.6 Hz, 6H); ¹³C NMR (75 MHz, CDCl₃) δ 163.7, 160.4, 147.4, 144.8, 135.9, 135.1, 134.0, 132.7, 129.1, 127.7, 127.6, 124.6, 121.3, 116.2, 115.9, 106.1, 53.5, 50.0, 41.3, 35.1, 28.3, 22.4. HRMS [ESI⁺] *m/z* calcd for C₂₁H₂₂FN₃O₂S [M+H]⁺: 400.1409, found: 400.1446.

5.2.3. 2-[1-(2,6-dichlorophenyl)-5-isobutyl-1H-pyrazol-3-yl)methyl]-2,3-dihydrobenzo[d]isothiazole 1,1-dioxide (**11**)

Yield; 74.0%; ¹H NMR (300 MHz, CDCl₃) δ 7.84 (d, *J* = 7.7 Hz, 1H), 7.62–7.30 (m, 6H), 6.40 (s, 2H), 4.57 (s, 2H), 4.38 (s, 2H), 2.24 (d, *J* = 7.3 Hz, 2H), 1.92–1.79 (m, 1H), 0.89 (d, *J* = 6.6 Hz, 6H); ¹³C NMR (75 MHz, CDCl₃) δ 148.3, 146.4, 135.4, 135.2, 135.1, 134.2, 131.0, 129.0, 128.8, 124.6, 121.4, 105.4, 49.6, 41.3, 34.8, 27.5, 22.5.

5.2.4. 2-[(1-(*tert*-Butyl)-5-phenyl-1H-pyrazol-3-yl)methyl]-2,3-dihydrobenzo[d]isothiazole 1,1-dioxide (**12**)

Yield 40%; ¹H NMR (300 MHz, CDCl₃) δ 7.86 (d, *J* = 7.5 Hz, 1H), 7.65–7.52 (m, 2H), 7.43–7.35 (m, 2H), 6.27 (s, 1H), 4.54 (s, 2H), 4.47 (s, 2H), 1.49 (s, 9H); ¹³C NMR (75 MHz, CDCl₃) δ 144.1, 143.5, 135.3, 134.3, 134.0, 132.5, 130.4, 129.0, 128.4, 127.8, 124.5, 121.5, 61.3, 50.0, 41.4, 31.2.

5.2.5. 2-[(1-(*tert*-Butyl)-5-(4-fluorophenyl)-1H-pyrazol-3-yl)methyl]-2,3-dihydrobenzo[d]isothiazole 1,1-dioxide (**13**)

Yield 42%; ¹H NMR (300 MHz, CDCl₃) δ 7.86 (d, *J* = 7.6 Hz, 1H), 7.65–7.53 (m, 2H), 7.41 (d, *J* = 7.5 Hz, 1H), 7.35–7.29 (m, 2H), 7.13–7.06 (m, 2H), 6.27 (s, 1H), 4.53 (s, 2H), 4.46 (s, 2H), 1.48 (s, 9H); ¹³C NMR (75 MHz, CDCl₃) δ 164.4, 162.3, 161.1, 143.6, 142.9, 135.3, 134.2, 132.6, 132.2, 132.1, 129.9, 129.0, 124.5, 121.5, 115.0, 114.7, 109.3, 61.3, 50.0, 41.3, 31.2.

5.2.6. 2-[(1-(*tert*-Butyl)-5-(4-trifluoromethylphenyl)-1H-pyrazol-3-yl)methyl]-2,3-dihydrobenzo[d]isothiazole 1,1-dioxide (**14**)

Yield 39%; ¹H NMR (300 MHz, CDCl₃) δ 7.85 (d, *J* = 7.7 Hz, 1H), 7.68–7.48 (m, 6H), 7.41 (d, *J* = 7.4 Hz, 1H), 6.29 (s, 1H), 4.54 (s, 2H), 4.47 (s, 2H), 1.49 (s, 9H); ¹³C NMR (75 MHz, CDCl₃) δ 143.9, 142.4, 137.9, 135.3, 134.2, 132.6, 130.9, 130.8, 130.5, 129.0, 125.7, 124.8, 124.7, 124.5, 122.1, 121.5, 109.4, 61.5, 50.1, 41.3, 31.3.

5.2.7. 2-[(1-(*tert*-Butyl)-5-(4-piperidin-1-yl-phenyl)-1H-pyrazol-3-yl)methyl]-2,3-dihydrobenzo[d]isothiazole 1,1-dioxide (**15**)

[1-(*tert*-Butyl)-5-(4-(piperidin-1-yl)phenyl)-1H-pyrazol-3-yl]methanol (54.9 mg, 0.18 mmol) was reacted with triphenyl phosphine (93.1 mg, 0.36 mmol) and carbontetrabromide (121 mg, 0.37 mmol) for 1 h. at 0 °C. Without purification, the reaction mixture was added to compound **8** (27.3 mg, 0.16 mmol) in DMF, and stirred for overnight. Then the reaction mixture was extracted with ethyl acetate. The organic layer was dried over magnesium sulfate, filtered, concentrated in reduced pressure, and purified by column chromatography (Hex: EtOAc = 4: 1 then 1: 1) to give title compound (15.2 mg, 20%).

¹H NMR (300 MHz, CDCl₃) δ 7.89 (d, *J* = 7.9 Hz, 1H), 7.64–7.52 (m, 2H), 7.40 (d, *J* = 7.1 Hz, 1H), 7.30–7.17 (m, 2H), 6.29 (d, *J* = 8.7 Hz, 2H), 6.22 (s, 1H), 4.52 (s, 2H), 4.46 (s, 2H), 3.26–3.23 (m, 4H), 1.79–1.74 (m, 4H), 1.67–1.63 (m, 2H), 1.49 (s, 9H); ¹³C NMR (75 MHz, CDCl₃) δ 151.9, 144.4, 143.3, 135.4, 134.3, 132.5,

131.1, 128.9, 124.5, 123.7, 121.4, 114.9, 109.0, 61.0, 50.0, 41.4, 31.2, 25.7, 24.3.

5.2.8. 2-[(1-(*tert*-Butyl)-5-(4-cyclohexylphenyl)-1H-pyrazol-3-yl)methyl]-2,3-dihydrobenzo[d]isothiazole 1,1-dioxide (**16**)

Yield 31%; ¹H NMR (300 MHz, CDCl₃) δ 7.83 (d, *J* = 7.5 Hz, 1H), 7.63–7.50 (m, 2H), 7.40 (d, *J* = 7.5 Hz, 1H), 7.30–7.20 (m, 4H), 6.24 (s, 1H), 4.53 (s, 2H), 4.45 (s, 2H), 2.56 (brs, 1H), 1.92–1.77 (m, 5H), 1.48–1.27 (m, 14H); ¹³C NMR (75 MHz, CDCl₃) δ 148.5, 144.3, 143.4, 135.4, 134.3, 132.5, 131.3, 130.3, 128.9, 126.2, 124.5, 121.4, 109.0, 61.1, 50.0, 44.3, 41.4, 34.4, 31.2, 26.9, 26.1.

5.2.9. 2-[(1-(*t*-butyl)-5-isobutyl-1H-pyrazol-3-yl)methyl]2,3-dihydrobenzo[d]isothiazol-1,1-dioxide (**17**)

Yield 79%; ¹H NMR (300 MHz, CDCl₃) δ 7.81 (d, *J* = 6.6 Hz, 1H), 7.60–7.48 (m, 2H), 7.36 (d, *J* = 7.4 Hz), 6.18 (s, 1H), 4.45 (s, 2H), 4.34 (s, 2H), 2.64 (d, *J* = 7.1 Hz), 2H), 2.09–1.09 (m, 1H), 1.64 (s, 9H), 0.98 (d, *J* = 6.6 Hz, 6H); ¹³C NMR (75 MHz, CDCl₃) δ 143.6, 143.1, 135.4, 134.3, 132.5, 128.9, 124.5, 121.3, 106.7, 59.9, 49.9, 41.4, 27.3, 30.5, 28.4, 22.7.

HRMS [ESI⁺] *m/z* calcd. for C₁₈H₂₇N₃O₂S [M + H]⁺: 362.1801, found: 362.1850.

5.2.10. 2-[(1-Isobutyl-5-phenyl-1H-pyrazol-3-yl)methyl]-2,3-dihydrobenzo[d]isothiazole 1,1-dioxide (**18**)

Yield 44%; ¹H NMR (300 MHz, CDCl₃) δ 7.86–7.63 (m, 1H), 7.63–7.51 (m, 2H), 7.49–7.37 (m, 6H), 6.42 (s, 1H), 4.56 (s, 2H), 4.41 (s, 2H), 3.96 (d, *J* = 7.5 Hz, 2H), 2.24–2.15 (m, 1H), 0.79 (d, *J* = 6.7 Hz, 6H); ¹³C NMR (75 MHz, CDCl₃) δ 145.9, 145.6, 136.8, 135.2, 134.0, 133.0, 132.6, 130.8, 129.0, 128.7, 124.6, 121.4, 106.1, 56.8, 49.9, 41.3, 29.6, 19.8.

5.2.11. 2-[(5-(4-Fluorophenyl)-1-isobutyl-1H-pyrazol-3-yl)methyl]-2,3-dihydrobenzo[d]isothiazole 1,1-dioxide (**19**)

Yield 62%; ¹H NMR (300 MHz, CDCl₃) δ 7.61–7.52 (m, 2H), 7.46–7.33 (m, 4H), 7.18–7.12 (m, 2H), 6.41 (s, 1H), 4.56 (s, 2H), 4.41 (s, 2H), 3.91 (d, *J* = 7.5 Hz, 2H), 2.26–2.08 (m, 1H), 0.80 (d, *J* = 6.7 Hz, 6H); ¹³C NMR (75 MHz, CDCl₃) δ 146.0, 144.5, 136.8, 135.2, 134.0, 133.0, 132.6, 131.0, 130.8, 129.2, 129.1, 124.8, 124.5, 121.4, 115.9, 115.6, 106.3, 56.7, 49.9, 45.7, 41.2, 29.6, 19.8.

5.3. Biological evaluation

5.3.1. *In vitro* evaluation of inhibitory activity against T-type calcium channel

High throughput assay (HTS) and electrophysiological recordings (whole-cell patch clamp assay) for T-type calcium channel inhibitory activity performed according to a previously described protocol.⁹

For FDSS binding assay: During the whole procedure, cells were washed using the BIO-TEK 96-well washer. The stably expressed T-type calcium channel in HEK293 cells was grown with puromycin (1 µg/mL), streptomycin (100 mg/mL), penicillin (100 U/mL), geneticin (500 mg/mL), and 10% (v/v) fetal bovine serum in modified Eagle's medium at 37 °C in a humid atmosphere of 95% air and 5% CO₂. Prior to using in a HTS FDSS6000 assay, cells were seeded in 96-well black-wall clear-bottom plates at a density of 4 × 10⁴ cells/well. Cells were incubated for 60 min at room temperature with 0.001% Pluronic F-127 in a HEPES-buffered solution composed of (in mM) and 5 mM fluo3/AM: 20 HEPES, 13.8 glucose (pH 7.4), 115 NaCl, 5.4 KCl, 0.8 MgCl₂, 1.8 CaCl₂. The increase in [Ca²⁺]_i by KCl-induced depolarization was detected. All data were collected and analyzed using the FDSS6000 and related software (Hamamatsu, Tokyo, Japan).

For IC₅₀ (half inhibition concentration of peak current) was determined, electrophysiological recordings (whole-cell patch

clamp assay) was performed by fitting raw data into dose-response curves according to previously described method.¹⁴ A standard whole-cell patch-clamp method was used. The current recordings were obtained using an EPC-9 amplifier and the Pulse/Pulsefit software (HEKA, Elektronik, Lambrecht/Pfalz, Germany). T-type Ca²⁺ currents were evoked every 15 s by a 50-ms depolarizing voltage step from –100 mV to –30 mV.

5.3.2. Evaluation of pharmacokinetic properties

The inhibitory activity of hERG channels and CYP450 enzyme, and metabolic stability in human liver microsomes were determined by following previously described method.⁹ Briefly, hERG channels inhibition of the synthesized compounds was determined using CHO-K1 Tet-On hERG cells purchased from IonGate Biosciences GmbH (Frankfurt, Germany), and IC₅₀ was performed as described for the patch-clamp method. Whole-cell recordings were analyzed using the Patchmaster/Fitmaster (HEKA Elektronik), IGOR Pro (WaveMetrics Inc., Portland, OR, USA), and GraphPad Prism 4 (GraphPad Software, Inc., La Jolla, CA, USA) software.

Inhibition of human CYP1A2, 2D6, 2C9, and 3A4 of tested compound was measured using the Vivid CYP450 kit (Invitrogen, Madison, WI, USA) according to the manufacturer's instructions. Briefly, the test compounds were diluted with water in a 96-well plate, followed by adding with the Master Pre-Mix (450 BACULOSOMES Regent and Regeneration system). The reaction was initiated by adding the Vivid CYP450 substrates and NADPH buffer after incubating of the mixture for 15 min at 37 °C. A fluorescence plate reader was used to measure the remaining enzyme activity. Positive controls were prepared by diluting solutions to 10 mM.

A metabolic stability assay of selected compound was performed by incubating human liver microsomes (HLM, UltraPool HLM 250 Mixed Gender Pooled Donor, Corning Gentest Co., Woburn, MA, USA) in the presence of NADPH (#44332000, Oriental Yeast Co., Tokyo, Japan) as the cofactor at 37 °C. Briefly, human liver microsomes were incubated with a 1 μM solution of the test compounds in potassium phosphate buffer (PPB) with the cofactor NADPH (1.2 mM) at 37 °C. Addition of cold acetonitrile containing 0.1 μg of internal standard after 30-min incubation was terminated the reaction. The supernatants were analyzed by LC-MS/MS, after removing precipitated protein by centrifugation.

5.3.3. In vivo efficacy test of diabetic neuropathic pain in streptozotocin (STZ) induced rat model

For the *in vivo* efficacy test for diabetic neuropathic pain, a STZ (streptozotocin)-induced neuropathic pain model was performed according to previously described methodology.¹⁵ Briefly, Rats (31) ensuring type 1 diabetes were induced by intraperitoneal injection of the diabetic drug STZ (65 mg/kg). 4 weeks after injection, the completely induced diabetic neuropathic pain rats (13) were selected by measured the blood glucose level and the pain

behavioral test. Mechanical allodynia was measured by von Frey according to previously reported methodology.¹⁶ The 6 rats were treated orally with 100 mg/kg of gabapentin, and the 5 rats were administered orally compound 100 mg/kg, the tests were evaluated at 1 h, 3 h, and 5 h. For mechanical allodynia tests,¹⁷ a von Frey filament (Stoelting, Wood Dale, IL, USA) was touched five times during every 3–4 s on the hind paw. For thermal hypersensitivity, the hargreave test was performed by beam. The frequency of paw withdrawal was expressed as a percentage [(No. of trials accompanied by brisk foot withdrawal/total No. of trials) × 100].

The results of behavioral tests, including both mechanical and thermal hypersensitivity, are expressed as % MPE. 100% MPE values near 100 indicate normal thresholds, whereas values near 0 indicate allodynia.

Acknowledgments

This research was supported by the KIST Intramural Program (2E26850) Brain Research Program through the National Research Foundation of Korea (NRF) funded by the Ministry of Science, ICT & Future Planning (NRF-2016M3C7A1913845) and the Original Technology Research Program (NRF-2016M3C7A1904344). Thanks for Dr. E. J. Lim and S. H. Seo for performing of *in vivo* efficacy test and pharmacokinetic experiments.

A. Supplementary data

Supplementary data associated with this article can be found, in the online version, at <http://dx.doi.org/10.1016/j.bmc.2017.07.008>.

References

1. Veves A, Backonja M, Malil RA. *Pain Med.* 2007;9:660.
2. Javed S, Petropoulos IN, Alam U, Malik RA. *Ther Adv Chronic Dis.* 2015;6:15.
3. Todorovic SM, Todorovic VJ. *Pflugers Arch Eur J Physiol.* 2014;466:701.
4. Latham JR, Pathirathna S, Choe WJ, Levin ME, Nelson MT, Lee WY, Krishnan K, Covey DF, Todorovic SM, Todorovic VJ. *Diabetes.* 2009;9:2656.
5. Messinger RB, Naik AK, Jagodic MM, et al. *Pain.* 2009;145:184.
6. Shin JB, Martinez-Salgado C, Heppenstal PA, Lewin GR. *Nat Neurosci.* 2003;6:724.
7. Berridge MJ, Lipp P, Bootman MD. *Nat Rev Mol Cell Biol.* 2000;1:11.
8. Bourinet E, Alloui A, Monteil A, et al. *EMBO J.* 2005;24:315.
9. Kim JH, Keum G, Jung H, Nam G. *Eur J Med Chem.* 2016;123:665.
10. Kerns EH, Di L. *Drug-like properties: Concepts, Structure design and methods from ADME to toxicity optimization.* Academic Press; 2008. chap.11:146.
11. Thompson AS, Humphrey GR, DeMarco AM, Mathre DJ, Grabowski EJJ. *J Org Chem.* 1993;58:5886.
12. Kim T, Choi J, Kwon O, Nah SY, Han YS, Rhim H. *Biochim. Biophys. Res. Commun.* 2004;324:401.
13. Leuranguer V, Mangoni ME, Nargeot RS. *J Cardiovasc Pharmacol.* 2001;37:641.
14. Choi KH, Song C, Shin D, Park S. *Biochim Biophys Acta.* 2011;1808:1560.
15. Wagner K, Inceoglu B, Dong H, et al. *Eur J Pharmacol.* 2013;700:93.
16. Khan S, Choi RJ, Lee J, Kim YS. *Eur J Pharmacol.* 2016;774:95.
17. Chaplan SR, Bach FW, Pogrel JW, Chung JM, Yaksh TL. *J Neurosci Methods.* 1994;53:55.